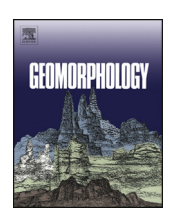


Contents lists available at ScienceDirect

Geomorphology

journal homepage: www.elsevier.com/locate/geomorph



Direct, continuous measurements of ultra-high sediment fluxes in a sandy gravel-bed ephemeral river



Kyle Stark ^{a,*}, Daniel Cadol ^a, David Varyu ^b, Jonathan B. Laronne ^c

- ^a Earth and Environmental Science, New Mexico Institute of Mining and Technology, Socorro, NM, USA
- ^b Technical Service Center, U.S. Bureau of Reclamation, Denver, CO, USA
- ^c Department of Geography, Ben Gurion University of the Negev, Be'er Sheva, Israel

ARTICLE INFO

Article history: Received 17 November 2020 Received in revised form 26 February 2021 Accepted 1 March 2021 Available online 94 March 2021

Keywords:
Bedload transport
Ephemeral
Suspended sediment
Gravel-bed river
Sediments

ABSTRACT

A dearth of field measurements exists from sandy gravel-bed rivers. Laboratory experiments suggest that sediment mixtures with a large sand component are particularly efficient at transporting bedload downstream. To evaluate transport processes in these environments, we constructed a sediment monitoring research facility with the ability to continuously monitor sediment fluxes. The Arroyo de los Pinos is a gravel-bed ephemeral channel with a large (>30%) sand component in New Mexico, USA. This field station incorporates direct measurements of bedload flux using Reid-type slot samplers with high quality measurements of suspended sediment, water depth, water velocity, and grain size. Measurements are collected at a stable cross section constructed for long-term, consistent monitoring.

Instantaneous bedload flux is high compared to global averages, as high as $12 \, \mathrm{kg \, s^{-1} \, m^{-1}}$. Suspended sediment is also high, peaking at $100,000 \, \mathrm{mg \, L^{-1}}$, with evidence of clockwise hysteresis. The Pinos nondimensional bedload flux rates are similar to those in other ephemeral channels, but the high sand content allows equal mobility at relatively shallow water depths and high rates of bedload transport during hydrograph recession. Bedload flux responded hysteretically, higher at equal shear stresses during stage rise. This is likely caused by an inadequate use of the depth-slope product for calculation of bed shear, steeper friction slopes during the rising limb, or both. These first monitored sediment transporting flash flood events reveal a channel that is very active during short periods of time. On average, the Arroyo de los Pinos flows $12-24 \, \mathrm{h}$ during $3-5 \, \mathrm{events}$ every year. However, in these brief periods, the channel is hyper-efficient at transporting bedload and suspended sediment at rates that are orders of magnitude higher than perennial counterparts.

© 2021 Published by Elsevier B.V.

1. Introduction

Ephemeral channels are ubiquitous in all climates but dominate the landscape in arid environments. Their role in sediment transport dynamics and landscape evolution are sometimes overlooked in favor of perennial systems, where sediment transport events are more prevalent. Large variations in sediment delivery are associated with ephemeral channels because of their highly variable and often flashy flows. In dryland environments, both arid and semiarid, sediment loads from ephemeral, unarmored tributaries are high when compared to global averages (Powell et al., 1996). Drylands cover 30% of Earth's land surface and are characterized by ephemeral channels that feed into few perennial trunk rivers. Direct field measurements of the total sediment discharge from these channels are limited: most data derive from gravel-dominated channels (Cohen and Laronne, 2005; Alexandrov

* Corresponding author. E-mail address: kyle.stark@student.nmt.edu (K. Stark). et al., 2009) or sand-bed rivers (Malmon et al., 2004; Billi, 2011; Lucía et al., 2013). There is a distinct lack of data from gravel-bed ephemeral channels with a high sand content (>30% sand). These sandy gravel-bed rivers tend to be matrix- rather than grain-supported, leading to higher bedload flux caused by lower inter-particle friction (Wilcock and Crowe, 2003; Miwa and Parker, 2017).

The discontinuity of flow in ephemeral channel networks leads to discrete, abrupt changes in the rates of sediment transport at river confluences. Many of the rivers in the western United States, especially in the arid southwest and central plains, have ephemeral tributaries that are the major source of sediment to the mainstem river. Current methods to calculate sediment load typically involve applying sediment transport equations for the particular field conditions of the channel. However, nearly all transport equations have been developed based on laboratory experiments or perennial systems (Gomez and Church, 1989). This makes applying these equations in ephemeral settings a dubious endeavor, especially because ephemeral streams can have an order of magnitude higher sediment load for a similar stream power when compared to perennial channels (Reid et al., 1995).

1.1. Previous sediment transport studies in ephemeral channels

Numerous datasets of suspended loads from ephemeral channels exist worldwide (e.g., Nordin, 1963; Lekach and Schick, 1982; Frostick et al., 1983; Sharma, 1996; Alexandrov et al., 2003; Achite and Ouillon, 2007; Nichols et al., 2008; De Girolamo et al., 2015). Suspended sediment concentrations (SSCs) are high in ephemeral channels because of the readily available sediment on largely unvegetated hillslopes. Clockwise hysteresis of suspended sediment is often present in suspended sediment-discharge relationships from ephemeral channels because of the discontinuous nature of flooding (Malmon et al., 2004). As with most perennial systems, suspended sediment is typically a large fraction of the total sediment load (Wolman and Miller, 1960; Alexandrov et al., 2009), although some research indicates equal rates of bedload transport in sand-bed rivers (Billi, 2011). Others have observed that the bedload/suspended sediment load ratio appears to increase with aridity (Anthony et al., 2001; Laronne and Wilhelm, 2001) and decreases with increased catchment size (Mathys et al., 2003).

Bedload transport monitoring has a more limited history. Bedload flux in semiarid regions is most often estimated through a series of proxy measurements between flood events. These can include scour chains, which determine the maximum amount of scour in a cross section (Hassan et al., 1999; Powell et al., 2005; Laronne and Shlomi, 2007), tagged particles, which estimate the movement of a given grain size downstream (Leopold et al., 1966; Hassan, 1993; Nichols, 2004) and sedimentation ponds, which capture the total sediment load and from which bedload is estimated assuming a certain grain size threshold (Martín-Vide et al., 1999; Nearing et al., 2007). Only a handful of studies have attempted direct, continuous measurements of bedload flux worldwide; even fewer of these are in desert climates. The Nahal Eshtemoa, the Nahal Yatir, and the experimental watershed at Walnut Gulch are three premier examples of locations where sediment transport studies have been undertaken in arid environments (Laronne et al., 1992; Laronne and Reid, 1993; Nichols et al., 2008). These channels are characterized by their unarmored bed and readily erodible bed material (Laronne and Reid, 1993) and are driven by high intensity rainfall that rapidly generates overland flow.

1.2. Sediment sampling equipment

Bedload measurement equipment has a long history of development. Most common are temporary bedload samplers deployed by the user and removed from the river once filled (Helley and Smith, 1971; Bunte et al., 2007). Among many others, these include Helley-Smith, Bunte traps, or mobile basket samplers. These samplers are generally ill-suited for ephemeral channels because of their limited capacity and inability to capture a wide range of grain sizes (Bunte et al., 2004). The most severe limitation of temporary samplers is the need for manual deployment during unpredictable and short-duration flash floods. Other methods of capturing bedload fall in the slot sampler category. These include vortex samplers (Milhous, 1973; Hayward, 1980; Tacconi and Billi, 1987), conveyor belt systems (Leopold and Emmett, 1976), and buried underground chambers (Reid et al., 1980). These systems are permanent and require considerable investment to construct and maintain. They are efficient at a wide range of transport rates and grain size distributions (Poreh et al., 1970; Habersack et al., 1998) and are designed to act as unobtrusive parts of the river bed. In previous studies of ephemeral channel bedload flux, the Reid-type (previously called the Birkbeck) slot sampler has customarily been used (Laronne et al., 1992; Cohen and Laronne, 2005; Lucía et al., 2011; Liébault et al., 2016; Zapico et al., 2018). Their use includes sand-bed channels, those with a high gravel content, small washes, and medium-sized watersheds.

Direct suspended sediment sampling has a more straightforward development history centering around two methods: grab sampling, where a sampler is deployed to a specific depth at a single location in

the river and vertically integrated sampling, where a sample is vertically integrated by sampling the entire column of water (Edwards and Douglas, 1999; Rai and Kumar, 2015). Both methods can be automated; automated grab sampling is more widespread. Recent comparability studies show an under-sampling bias when using the grab sampling method and that vertically integrated sampling is preferred (Groten and Johnson, 2018). Turbidity is the most prevalent indirect, or surrogate, measurement of suspended sediment. It is defined as an expression of the optical properties of a liquid that causes light rays to be scattered and absorbed rather than transmitted in straight lines through a sample. These measurements are then calibrated to discrete samples of suspended sediment to determine a relationship between turbidity and SSC. The generated rating curves are site specific and equipment specific (Davies-Colley and Smith, 2001).

1.3. Hypotheses

In this study we present a new dataset of bedload and suspended load transport from a sandy gravel-bed ephemeral channel in New Mexico while evaluating three hypotheses:

- Bedload flux in ephemeral, sand-rich gravel-bed channels is high compared to perennial systems. Bedload flux is expected to exceed that of other ephemeral channels at low shear stresses when the grain size distribution of the channel bed material promotes easier grain entrainment.
- Bedload flux and grain size vary across the channel, primarily because of sediment characteristics and geometry of the approach reach, particularly so in the shallow, most frequent bedload transporting events.
- 3. Investigating the grain size of both suspended sediment and bedload will reveal the transition of the sand fraction from being transported in bedload to suspended load. Based on previous research, individual classes of sand will probabilistically transition from bedload to suspension at predictable shear stresses.

2. Site description, equipment, and methods

2.1. Study area

The Arroyo de los Pinos (drainage area = 32 km²), chosen as the site for this study of sediment flux in the Southwest U.S., is a direct tributary to the Rio Grande and drains typical geologic formations in the middle Rio Grande Valley (Fig. 1). The setting varies throughout the basin (Cather and Colpitts, 2005); near the Rio Grande, the channel is anastomosing as it crosses Pliocene and Pleistocene ancestral Rio Grande floodplain and alluvial fan deposits. Farther upstream the channels are relatively confined through canyons and valleys eroded into the more cohesive early Paleozoic sandstones, limestones, and shales. The Abo formation (Permian) consists of interbedded mudstone, shale, and sandstone; the Bursum formation (Permian) consists of interbedded dolomitic limestone and sandstone; and the Atrasado formation of the Madera Group (Pennsylvanian) consists of limestone, arkosic sandstone, and mudstone (Cather and Colpitts, 2005). A geologic map of the Pinos is included as supplementary material.

The Pinos is located at the northern extent of the Chihuahuan Desert. This desert is semiarid; it has a mild continental climate characterized by low annual precipitation, year-round sunshine, and relatively large annual and diurnal temperature changes (WRCC, 2013). Average annual precipitation is 237 mm. July and August are the rainiest months; 35% of annual precipitation falls during these 62 days during brief, but intense storms. During the summer, atmospheric moisture is delivered to the region via the Gulf of California, with some higher atmospheric moisture also drifting inland from the Gulf of Mexico (Adams and Comrie, 1997). As moist air moves into the area strong surface heating combines with orographic uplift to form monsoonal storms (WRCC,

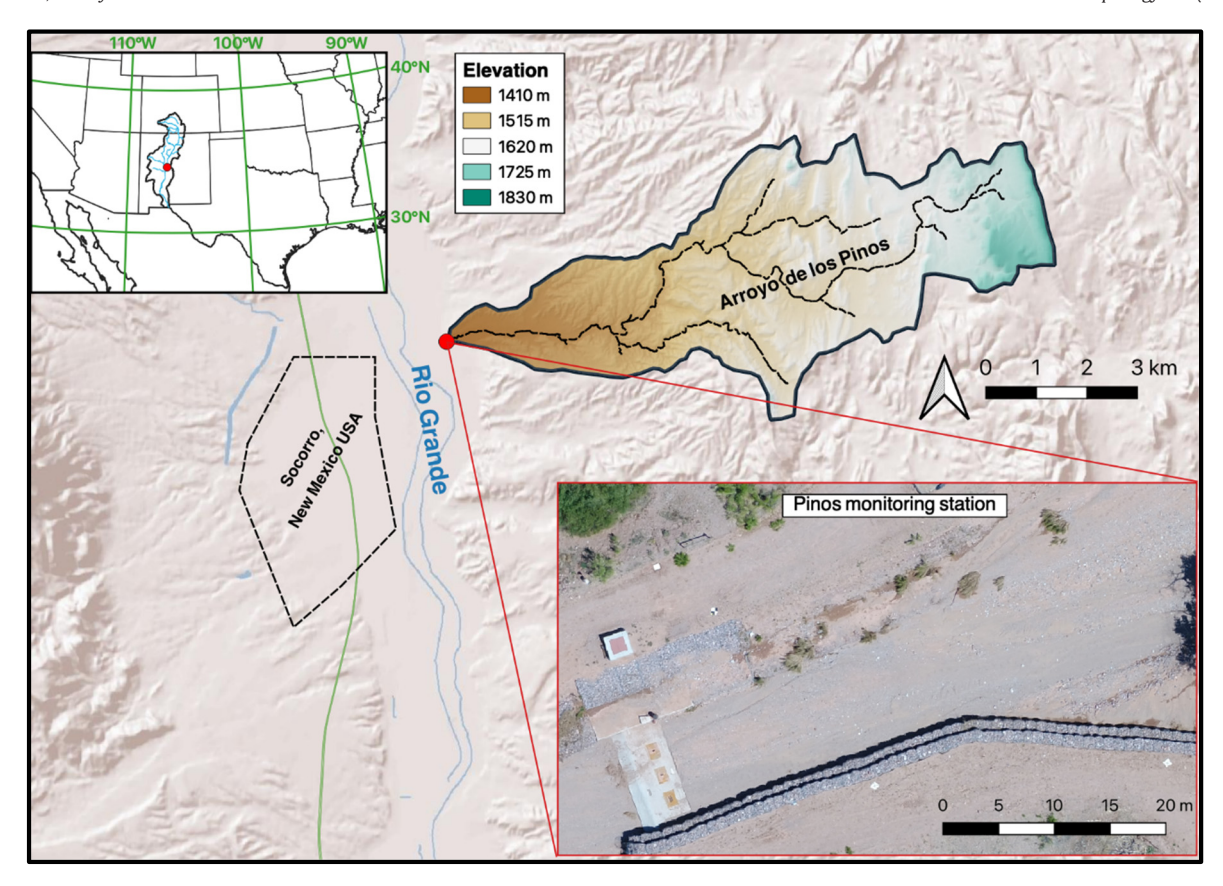


Fig. 1. Top left: location of the Pinos watershed (red dot) in the upper Rio Grande catchment (black outline). Center: Arroyo de los Pinos, the main channel network and the local elevation. Bottom right: drone imagery of the Pinos station and the approach reach.

2013). Winter precipitation derives from frontal activity of Pacific Ocean storms moving eastwards. These events are slow-moving and low-intensity, usually insufficient to cause flash floods like those during summer.

The intensity and duration of highly variable and localized rainfall are the primary controls on runoff generation (Belachsen et al., 2017; Marra and Morin, 2018). In addition, the position of the storm centroid relative to the watershed extent and storm cell velocity are additional

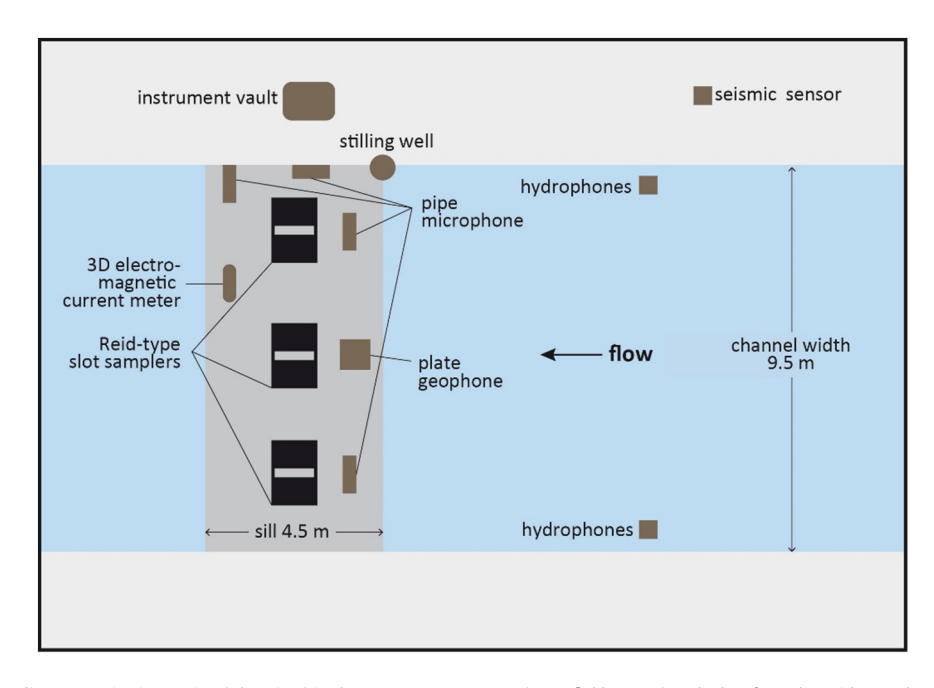


Fig. 2. Schematic of the Pinos sediment monitoring station (plan view) in the current arrangement (2020 field season). Only data from the Reid-type slot samplers have been used in the present manuscript for characterizing bedload flux.

important factors controlling runoff generation specific to semiarid climates (Morin and Yakir, 2014). Second order factors include the vegetation and pedology of the region. The positive feedback of infiltration capacity and biotic processes is well documented in arid ecosystems (Tongway et al., 2001; Saco et al., 2007). In these environments the presence of vegetation increases infiltration. Typical New Mexican summer storms are several kilometers in areal extent but have high rainfall intensities, frequently surpassing 30 mm h^{-1} for tens of minutes concentrated at the storm centroid.

Construction of the new sediment monitoring facility was completed in early 2018 (Figs. 2 and 3). The channel sides were stabilized using gabion baskets and a concrete wall. The channel bed was stabilized with a 15 cm thick concrete sill designed to have a 1.5% slope, similar to the local channel gradient. A concrete bench located on the right bank is used for staging equipment and sampling during smaller flow events. A large, concrete vault sits atop a levee directly adjacent to the channel. This houses the Yamma-designed computer and telemetry equipment required to process, store and automatically upload data to servers provided by Ayyeka Technologies. Data collection is triggered by a threshold stage of 5 cm, and data are uploaded via the cellular network every 30 min during flooding. To the best of our knowledge this is the first system to cellularly upload bedload data in real time.

To characterize the sediment available for transport (Fig. 4), we measured the b-axis of three hundred particles from the channel thalweg and two hundred particles each from two separate bars located 30 and 75 m upstream of the monitoring site. These pebble counts were truncated at 2 mm, with anything smaller binned together as fine material. To estimate the distribution of the sand and fine fraction, two bulk surface samples from the thalweg were sieved. To assess the grain size distribution of the subsurface (>5 cm depth), five bulk samples were

collected from the channel thalweg and six from bar locations. These two techniques (grid-by-number and sieve-by-weight) produce comparable results (Kellerhals and Bray, 1971) and were combined to assess the total distribution of grains within the Pinos channel.

The surface D_{50} of samples from the thalweg and bar were 5 and 14 mm, respectively. Sand comprised 34% of the thalweg and 15% of bars by mass, while silt and clay-sized material was typically less than 2.5%. The Pinos has an unarmored bed; samples of the thalweg surface (<5 cm depth, corresponding to the D_{98} of the surface) and subsurface show little difference in grain size distribution. The D_{50} of the surface samples was 5 mm while the subsurface was 6 mm. This is in agreement with studies of other ephemeral channels (Powell et al., 2012; Reid et al., 1995). In contrast, bar surface sediment is somewhat preferentially sorted relative to subsurface material. The bar surface D_{50} was 14 mm while the subsurface was 10 mm. The full grain size distribution of individual samples of channel material is provided as supplementary material alongside average grain size characteristics of the bedload material.

2.2. Instrumentation and data collection

The heart of the sampling system is three Reid-type slot samplers. These samplers operate using two pressure transducers (SEBA DS-22; $\pm 0.05\%$ accuracy) that enter each concrete pit via a buried conduit. One transducer is connected to a pressure pillow recording the combined pressure of bedload accumulating in the stainless-steel inner box and the water column above it, while the other monitors the pressure associated only with the water column. The equipment at the monitoring site, including pressure transducers, has a one-minute sampling frequency. A cover protects the sampler and remains flush with the bed surface. Sediment enters the sampler through a slot (30 cm length; 11



Fig. 3. Photos of constructed Pinos site in oblique view (A), looking upstream (B) and looking downstream (C).

cm width) in the cover. The slot width was determined after assessing the bed material; 11 cm is larger than the b-axis of any sediment found in the channel thalweg and larger than 99% of the material analyzed from bars. As sediment accumulates, these data are recorded simultaneously, such that the total bedload flux into the slot sampler is continuously monitored.

After a flow event, the steel boxes are lifted from the inner chamber and sediment is sub-sampled (see photos in supplemental material). Sediment fills the sampler from bottom to top, such that the sample taken from the top of the sampler is from the end of the sampling period. There is evidence that sediment accumulates as a cone, hence sampling from the center of the sampler preserves the sequential deposition of the sediment (Laronne et al., 2003). The volume of each sampler is 0.49 m^3 (length: 1.01 m, width: 0.6 m, height: 0.8 m), holding up to \sim 850 kg of sediment. Bedload samples were collected from the center of the sampler in 0.1 m-thick layers. Each sample was air dried before sieving in a large sieve (50 cm) set at roughly 1/2 phi intervals, and the largest grain (D_{max}) was measured and weighed separately. Grain size statistics were calculated using GRADISTAT (Blott and Pye, 2001).

Suspended sediment concentration was also measured in the Pinos. Two pressure transducers and two liquid level actuators were placed in a stilling well on the right bank (Fig. 2). Two protective perforated pipes extend sub-horizontally from the stilling well to 6 and 43 cm above the sill; each inlet houses one turbidity probe and one automated pump sampler intake (Teledyne, 2019). The actuators in the well trigger the automated pump samplers (grab samples); both samplers are activated at the same stage, even if the higher inlet is not submerged in water. This ensures that the samples are collected contemporaneously, allowing for direct analysis of the vertical stratification of suspended sediment. Depth-integrated manual sampling of suspended sediment was also conducted using DH-48 samplers to augment the pump samplers and allow for cross-stream comparison.

Manual measurements of water depth and velocity were collected using an electromagnetic velocimeter (Hach 950). These measurements were used to estimate discharge and to develop a rating curve at low water depths. At higher water depths (above ~30 cm in the Pinos), wading into the flood is too dangerous and remote estimates of velocity are required.

2.3. Data processing

Contemporary cross-sectional average bed shear stress was estimated for uniform, steady flow by the depth-slope product, $\tau = \rho_w gRS$, where ρ_w (kg m $^{-3}$) is water density, g (m s $^{-2}$) is the acceleration due to gravity, R (m) is hydraulic radius, and S is bed slope. The critical shear stress (τ_c), occurs at the initiation of motion, when grains begin to move owing to tractive forces. As shear stress increases, coarser grain sizes become mobile. We evaluated the mobility of each grain size class using transport stage, which allows us to evaluate shear stress relative to the critical shear stress (τ/τ_c).

The accumulated submerged weight within each sampler was calculated every sampling period (every 1 min) by subtracting the overlying water column weight using the co-located pressure transducer and transforming the pillow sensor output to accumulated sediment mass using the linear relationship from calibration. To find this relationship, each Reid-type sampler is empirically calibrated yearly. Known masses of sediment are added sequentially and the sensor response is recorded. Sediment input mass is varied to mimic the wide range of bedload flux that a given sampler may experience. The samplers are quite sensitive to changes in sediment mass, consistently able to measure incremental increases of 3–5 kg.

During flooding, sediment mass within the samplers accumulates at a highly variable rate. As such, longer term averages of sediment flux cause underestimation of the maximum flux rates that occur in short time frames. To overcome this, we have adopted a mass-averaging approach (Halfi et al., 2020). Rather than reporting mass accumulation at

a constant time step, this averaging methodology reports data at a constant mass step, or mass threshold. Once the threshold is exceeded, mass is evaluated against the time required to achieve the threshold such that:

$$q_b = \frac{1}{L} \frac{\Delta M}{\Delta t} \tag{1}$$

where q_b (kg s⁻¹ m⁻¹) is bedload flux at the location of the sampler, ΔM (kg) is the mass accumulated in the sampler, L (m) is the width of the slot, and Δt (s) is the time required to exceed the mass threshold, in minute intervals (i.e., $\Delta t = 60$ s, 120 s). The mass averaging technique is dynamic; it can precisely calculate high bedload fluxes (above 10 kg s⁻¹ m⁻¹) as well as low bedload fluxes (below 0.01 kg s⁻¹ m⁻¹) by changing the time averaging interval. This helps accommodate the sensitivity of the pressure pillow and transient pressure fluctuations caused by turbulence. The mass threshold used in this study was 5 kg, chosen because it corresponds to a conservative lower limit for a measurable amount of sediment in the sampler.

To assess how data collected from the Pinos compare with that from other channels, we nondimensionalized our data. Nondimensional transport rates are presented using the Einstein transport parameter (Einstein, 1950):

$$q_b^* = \frac{q_b}{\rho_{sed} \sqrt{g D_{50}^3 \left(\frac{\rho_{sed} - \rho_w}{\rho_w}\right)}}$$
 (2)

and nondimensional shear stresses are represented using the Shields number (Shields, 1936):

$$\tau^* = \frac{\tau}{g(\rho_{\text{sed}} - \rho_w)D_{50}} \tag{3}$$

where ρ_{sed} is sediment density (2650 kg m⁻³). The surface median grain size is used for D_{50} , and τ is contemporary reach averaged shear stress.



Fig. 4. Pinos side view of bar (A) and thalweg (B) sediment. No evidence of armoring is found in thalweg material while slight armoring is evident in bars.

3. Results

Data from nine flow events are presented in this paper (Table 1). Monitoring of the Pinos began in 2016, but the first significant flow events occurred in 2017 and construction of the principal monitoring station was completed in 2018. As such, bedload data are only available from 2018 onward. The peak water depth of the events ranged from 15 to 161 cm. Researchers were present on-site during eight of the nine events and undertook manual measurements of suspended sediment and velocity to augment the data monitored by the automated systems. Bedload flux measured by the Reid-type samplers was high (maximum 12 kg s⁻¹ m⁻¹) while maximum suspended sediment concentrations surpassed 100,000 mg L⁻¹ (Figs. 5 and 6). For larger floods (2018-07-26 and 2018-08-24) the samplers filled within 30 min, sampling a small fraction of the flow event. Critical shear stress was estimated to be 4.7 Pa (τ_c^* , the nondimensional critical shear stress [Eq. (3)] is estimated to be 0.06), based on the initiation of motion monitored by the three slot samplers. Values of τ_c ranged from 4.7 to 5.2 Pa for all nonbore flow events for all samplers.

Suspended sediment data collected in 2017 (prior to construction) were compared to those collected in 2018 with no observed significant

Table 1Summary of flow events monitored in the Pinos. Flow events during 2017 occurred prior to construction of the principal monitoring station.

Event date	Flow duration (hours)	Peak 15-minute rainfall intensity (mm 15-min ⁻¹)	Maximum water depth (cm)	Reach-average max bedload flux ^a (kg s ⁻¹ m ⁻¹)	Max SSC (mg L ⁻¹)
2017-07-15	2.5	10.4	55	_	64,000°
2017-07-22	2.75	11.1	33	_	74,700 ^c
2017-09-27	2.5	5.1	28	_	49,100 ^c
2017-10-05	3.5	6.1	60	-	51,000 ^c
2018-07-16	3.00	15.1	60	-	104,000
2018-07-26	5.50	28.5	161	12.0 ^b	-
2018-08-09	1.75	5.8	17	4.0	29,600
2018-08-24	2.75	7.2	32	12.0	90,100
2018-09-01	5.50 (two storms)	7.5	15	1.0	34,500 ^c

^a Reach-averaged bedload flux is measured directly using Reid-type slot samplers. All bedload flux data were calculated in the shortest possible timestep (60 s).

^c Manual, vertically integrated suspended sediment sample.

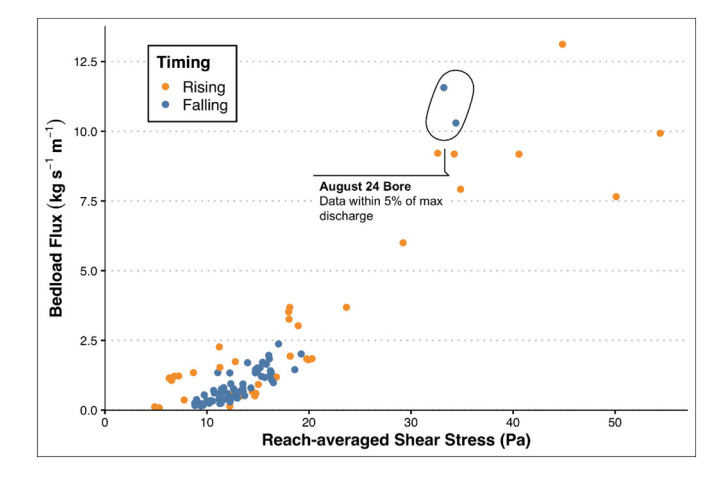


Fig. 5. Reach-averaged bedload flux with respect to shear stress. Bedload flux is measured using the average of Reid-type slot samplers.

difference; this indicates that construction of the site had little effect on suspended sediment delivery through the monitored cross section. Using both datasets we evaluated the variability of suspended sediment concentration with timing of sampling. The SSC of samples collected during hydrograph recession varied linearly with water depth, while the SSC of samples collected during hydrograph rise and peak flow follow a separate trend (Fig. 6).

Bedload grain size distribution was determined by subsampling sediment captured by the Reid-type slot samplers (Fig. 7). Most of the samples exhibited either a bimodal (56%) or unimodal (24%) distribution. A typical bimodal distribution had peaks between 1–3 mm and 8–10 mm. Unimodal distributions typically preserved one of these two peaks, with samples collected during low discharges preserving the sand mode (1–3 mm) and samples collected at high discharges preserving the gravel mode (8–10 mm). These bedload data were evaluated against shear stress (Fig. 8). With the exception of the 2018–08–24 event (a borestyle flood that filled the samplers in less than 10 min) reach-averaged bedload D_{50} increased with reach-averaged shear stress to a maximum of ~5 mm at 17 Pa. Above 17 Pa the D_{50} did not change substantially. The trend between D_{90} and reach-averaged shear is similar. At $\tau > 17$ Pa, D_{90} did not significantly increase (Fig. 8).

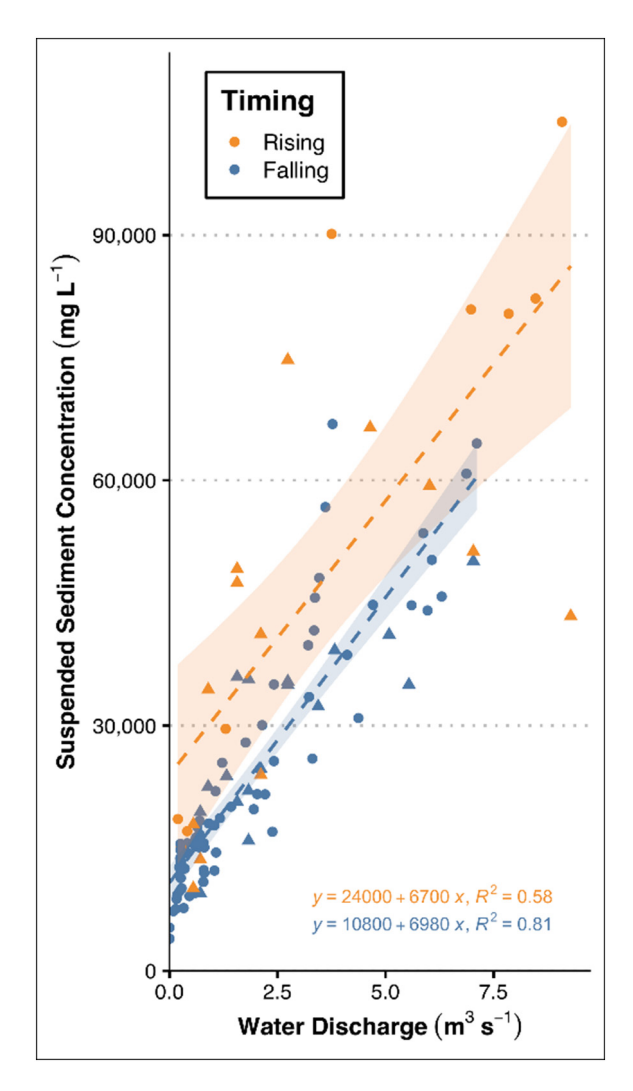


Fig. 6. Suspended sediment concentration with respect to water discharge, colored by hydrograph location. The dashed lines represent a simple linear fit to the data (orange, data collecting during hydrograph rise; blue, data collected during hydrograph recession). The shaded regions are 95% confidence bands of the linear models. *P*-values for both regressions are <0.0001. Triangles are samples collected in 2017 and circles are samples collected in 2018.

^b Peak bedload flux recorded before maximum water discharge was achieved.

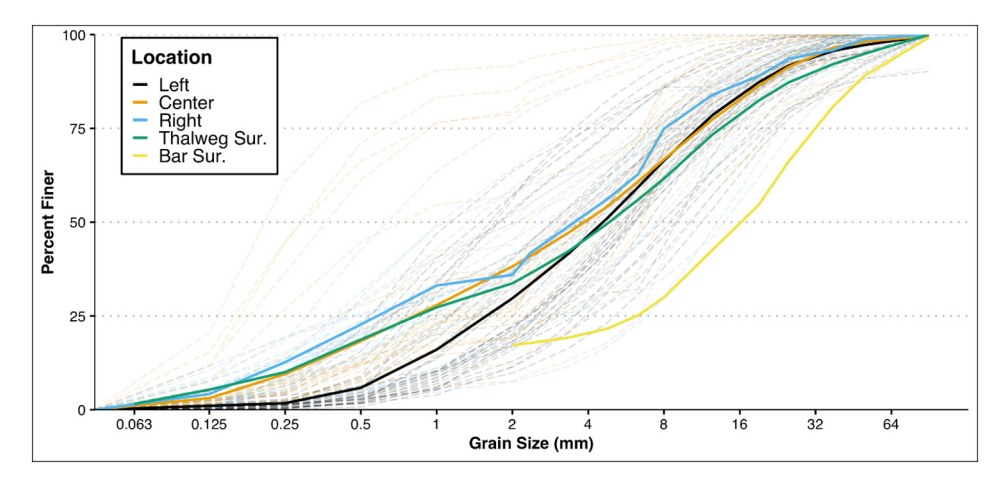


Fig. 7. Grain size distribution of samples collected from the left sampler, center sampler, right sampler, thalweg surface material, and bar surface material. Individual samples are indicated by faint dashed lines (left, right, and center bedload samples only), averages are indicated by thick solid lines.

For the 2018-07-16 flow event, the first following site construction, bedload flux and median grain size were abnormally low for the measured shear stresses. Large excavators and other construction equipment working in the approach reach likely compacted the bed, thereby temporarily and artificially decreasing bedload fluxes. Hence, data from this flow event were useful for testing the station, but may not represent typical conditions in the Pinos. Because of this unnatural state of the river, these data are excluded from analysis.

4. Analysis and discussion

4.1. Bedload transport and grain size variation

The Pinos dataset is unique because of the high sand content of the channel; 34% of non-bar sediment is sand. This high percentage of sand allows for easier transport of both sand and gravel (Wilcock et al., 2009). Full mobility (when all grain size classes are mobile) is achieved at very low transport stages – some portion of all grain sizes is active near τ_c (Fig. 9). Equal mobility, when all grain size classes are proportionally represented in the bedload sample, is achieved between

14 and 23.5 Pa $(3\tau_c - 5\tau_c)$. The specific shear stress when equal mobility occurs is difficult to estimate given the lack of data in this range, but samples collected below 14 Pa show high proportions of sand and fine gravel, relative to channel thalweg material and above 23.5 Pa the distribution of grain sizes is better approximated by surface bar material. Sediment from bars is much coarser than in the thalweg. This sediment requires a higher stage to inundate and higher shear stresses to activate. Consequently, full mobility of bar material occurs at higher shear stresses than are presented in this paper. In addition, bedload D_{50} and D_{90} are invariant above 17 Pa (3.6 τ_c - Fig. 8), suggesting that equal mobility is achieved approaching this shear stress. The D₅₀ of bedload samples also matches that of surface channel thalweg material at this shear stress (5 mm). This estimation of equal mobility matches similar estimates of equal mobility measured in gravel bed rivers. Powell et al. (2001) estimated equal mobility at $4.5\tau_c$ in the Nahal Eshtemoa, a channel with a much smaller sand fraction (~10% sand) and loess banks that prevent bank erosion and provide a very stable channel. Laboratory experiments often have lower thresholds for equal mobility associated with the breakup of an armor layer or dominant discharge (Parker, 1978; Wilcock and McArdell, 1993). Equal mobility in the Pinos likely

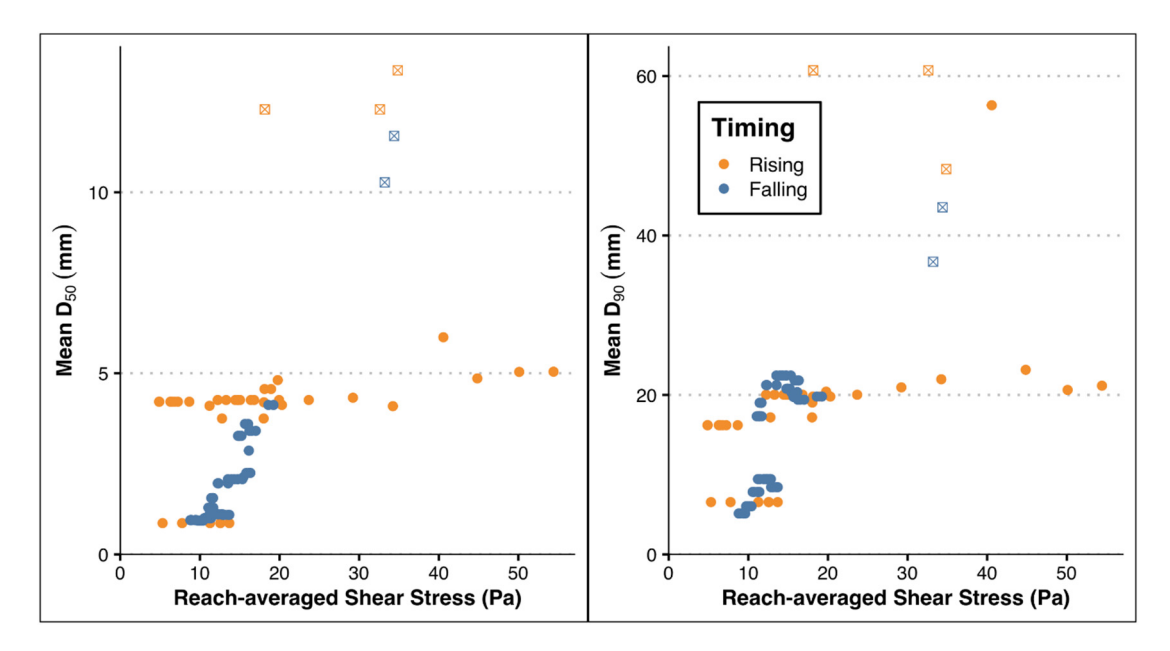


Fig. 8. Variation of bedload D₅₀ and D₅₀ grain size with increasing shear stress. Samples that are hollow boxes are from the 2018-08-24 bore-style flow event.

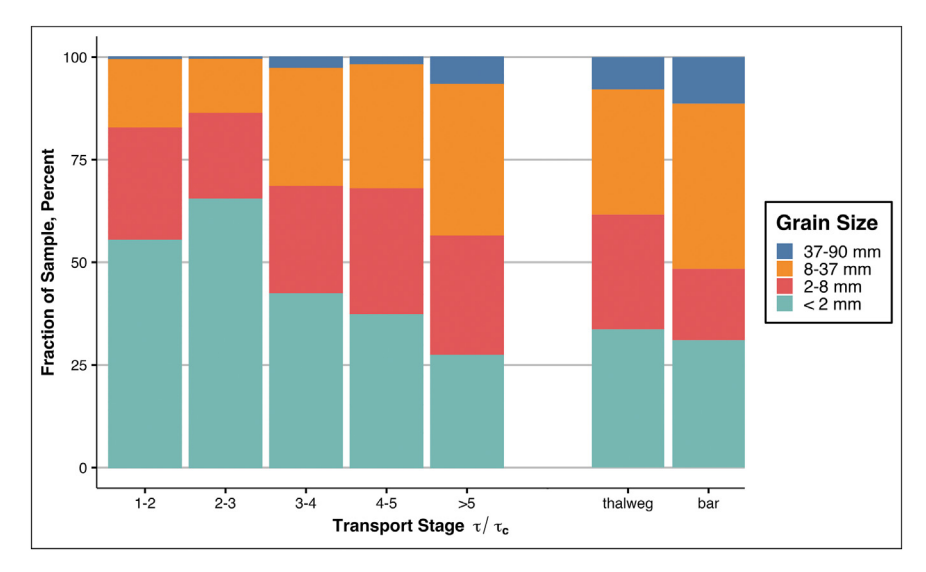


Fig. 9. Grain size distribution of samples collected at various transport stages (τ/τ_c) compared to the distribution surface thalweg and bar material.

occurs at a shear stress in between these published values because of its large sand fraction. The absolute value of critical shear stress (identified using Reid-type slot samplers) is very low because all sediment classes are more mobile with a sediment mixture such as the Pinos (Wilcock and Crowe, 2003). Therefore, equal mobility is achieved at higher ratios of critical shear stress. Our measured value of critical shear stress (4.7 Pa) equates to a critical Shields number (τ_c^*) of 0.06, which is similar to globally reported values for gravel-bed rivers (Buffington and Montgomery, 1997; Recking, 2009).

Bedload flux across the channel varied significantly; the left Reidtype slot sampler filled 2–3 times faster than the sampler located closest to the right bank. Additionally, average grain size distribution of bedload samples collected from the right and center sampler are finer-grained in comparison to samples collected from the left sampler (Fig. 7). Specifically, samples collected from the left sampler had larger fractions of fine and medium gravel (4–16 mm). This is likely because of the position of the thalweg in the approach reach. In 2018, a deep, confined thalweg formed on the left bank in the immediate area upstream of the samplers, while a small bar formed immediately upstream of the center sampler. This promoted preferential bedload flux of gravel-sized sediment along the left bank of the channel.

The largest grain sizes are somewhat underrepresented in bedload samples (Fig. 9). We hypothesize two reasons for this disparity. First, slot sampler efficiency decreases as the grain size approaches the slot length and width (Poreh et al., 1970). The largest grain sizes are sampled slightly less efficiently than the sand and small gravel classes, which may contribute to this disparity. Second is a potential undercollection of large grains in the center of the sampler chamber under the sampler slot. Although this phenomenon was tested and not observed in other channels (see Bergman et al., 2007), informal observations at the Pinos suggests that larger grains may accumulate preferentially in the corners of the slot sampler by rolling farther than finer sediment on the sloping sides of the sediment cone. We gathered samples for sieving from the center of each sampler. This hypothesis will be tested in future flow events by conducting extra sampling to determine if sediment gathered from the corners of the box differs systematically from that gathered from the center. The largest size classes (>37 mm) include only a few individual grains in each sample, so a consistent difference of only one or two grains may be significant.

A positive correlation exists between bedload flux and reachaverage shear stress (Fig. 5). Using linear regression analysis, we find that the data collected during hydrograph rise and hydrograph recession have a similar coefficient of determination ($R^2=0.82$ and

0.83, respectively). However, there are noticeable differences between the two segments of the hydrograph. When evaluating the temporal changes in bedload flux, the largest instantaneous bedload fluxes and largest grain sizes occur during the rising limb or near peak discharge (Figs. 5 and 8). Median grain size is also larger during the rising limb $(D_{50 \text{rising}} = 4.7 \text{ mm vs } D_{50 \text{recession}} = 1.8 \text{ mm})$. This behavior is specifically evident in bore style floods (i.e., the 2018-08-24 event), when peak discharge is attained within minutes. These departures from a trend may be associated with a change in near-bed turbulence. Higher turbulence has been measured during the rising limb of hydrographs in ephemeral channels (Halfi et al., 2018). These rapid changes in turbulence are not captured by traditional means (i.e., depth-slope product of shear stress) and highlight drawbacks of using this method in sediment transport studies (Biron et al., 2004; Yager et al., 2018). These dynamic changes in shear stress are characteristic of ephemeral settings because of their flashy nature. Another consideration is the hysteretic nature of water surface slope. We approximate the water surface slope using the bed slope. Water surface slope is generally clockwise hysteretic and is higher during the rising limb of a hydrograph (Meirovich et al., 1998). This should account for some of the observed differences between the rising and falling limbs of the hydrograph. Based on these and other (e.g., Mrokowska and Rowiński, 2019) results, shear stress is likely different for a given water discharge through the course of a flood, especially during quick rising bore-style floods. In this study, we evaluate our findings using the more traditional estimates of shear stress to directly compare our data to that from other channels. We recommend future studies on the Pinos and other flood-driven channels should consider methods to better estimate how local bed shear stress changes throughout a flood hydrograph, among others by measuring turbulent fluctuations of water velocity.

One lingering concern is that the measured cross section, an artificially narrowed 9.5 m wide channel, differs substantially from upstream cross sections, which have wide (20–50 m) anastomosing and braided reaches. The channel was narrowed more than 60 yr ago and inspection of the bed before and after events suggests that the channel has achieved a dynamic equilibrium. As such, measured sediment flux within the monitored cross section is the same as elsewhere in the lower reaches of the watershed. Additionally, depth-slope shear stress will also be similar as long as flow is confined to the main thalweg of the channel. Notably, 90% of bedload flux, grain size distributions, and shear stresses presented here derive from periods of time when flow was fully contained in this deepest part of the channel.

4.2. Suspended sediment flux and mechanisms of sand transport

A rating curve is available for water discharge below 7.5 m³ s⁻¹. Suspended sediment concentration varied linearly with water discharge (Fig. 6). When evaluating transport via suspension, concentration differences between hydrograph rise and recession become apparent; suspended sediment sampled on the rising limb are roughly twice as concentrated when compared to similar discharges during hydrograph recession. The correlation between concentration and discharge is also much stronger after peak flow (R² = 0.81) than before it (R² = 0.58). Unlike the bedload dataset, there is a clear scientific basis for this phenomenon. The clockwise hysteresis in suspended sediment concentration has been attributed to the availability of fine sediment from channel banks and hillslopes during the initial rise (Alexandrov et al., 2003; Malmon et al., 2004).

Using these data, we also estimated material flux across the channel for both suspended load and bedload. Globally, suspended load accounts for a majority of total sediment load in ephemeral channels (Wolman and Miller, 1960; Alexandrov et al., 2009). In contrast to most previous studies, bedload flux was similar in magnitude to suspended sediment flux for small discharges in the Pinos (Fig. 10). This is especially relevant when considering flood frequency: in four years of monitoring the Pinos (two of which, 2016 and 2019, recorded no significant flow at the monitoring station), all but three events had maximum discharges below 10 m³ s⁻¹ and a majority peaked below 5 m³ s⁻¹. As water discharge increases in the Pinos, there is an exponential increase in the suspended sediment load, thereby decreasing the ratio of bedload to suspended load. This change is driven by sand transitioning from bedload to suspension (Fig. 11).

These high bedload/suspended ratios at low water discharges (Fig. 10) are perhaps the most surprising set of results. Reported bedload/suspended load ratios range between 0.05 and 0.25, depending on the type and size of a flood (Wolman and Miller, 1960; Sadeghi and Kheirfam, 2015). The Pinos has a ratio near 1.0 at low discharges. This is because of the high sand content of the channel and the low content of silt and clay in the basin. Fine and medium sand (0.063–0.50 mm) are transported as bedload at low discharges, but gradually move into suspension as discharge increases (Fig. 11). Hence, up to 25% of the transported sediment (the fraction of the bed that is fine and medium sand) transitions from traction to suspension. This transition produces a commensurate increase of sand in the suspended material load: 10% of sediment in suspension is sand at 0.5 m³ s⁻¹ while sand makes up 20% of transported sediment at 3.5 m³ s⁻¹. These dynamics are

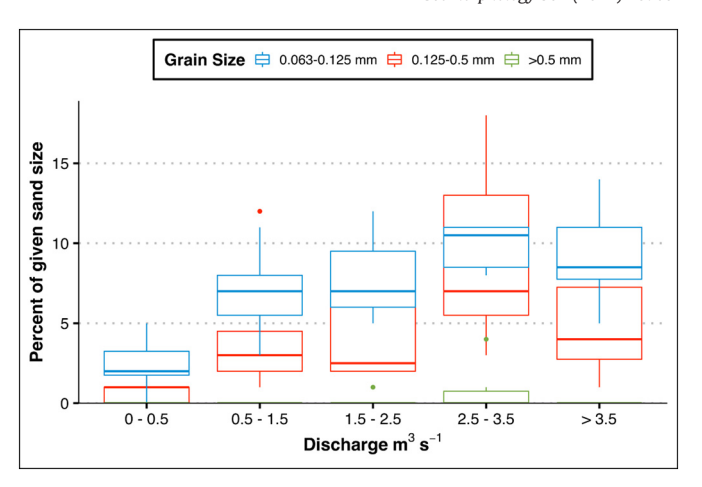


Fig. 11. Sand fraction of suspended sediment. An increase in the 0.063–0.5 mm size class is observed while less change in the larger (>0.5 mm) size class.

particularly important for river managers, who can use sediment flux ratios combined with measurements of suspended sediment to estimate total loads from tributary channels such as the Pinos.

4.3. The Pinos in a global context

Measured bedload fluxes are much higher in the Pinos compared to perennial systems – but are similar to other ephemeral channels – for all shear stresses presented in this study (Fig. 12). This analysis is a complement to a comparison of the Nahal Yatir, an ephemeral channel in Southern Israel, to perennial channels worldwide (Reid et al., 1995). Here, we have included data from the Pinos and two additional channels for a total of nine sites with monitored bedload discharges. Slot samplers were deployed as a sampling mechanism in all these rivers and cover a wide range of climates: from arid (Yatir, Eshtemoa, and Pinos) to temperate (East Fork, Turkey, and Goodwin), and mountainous/grassland or wooded regions (Caspar, Oak, and Torlesse). Table 2 provides a summary of the characteristics of each stream. Each dataset is presented in nondimensional space (data were nondimensionalized using Eqs. (2) and (3)) in an attempt to directly compare the rivers.

The Pinos bedload flux data are similar to those from other ephemeral channels over the range of measured shear stresses (Fig. 12). In nondimensional space, these channels form an upper envelope,

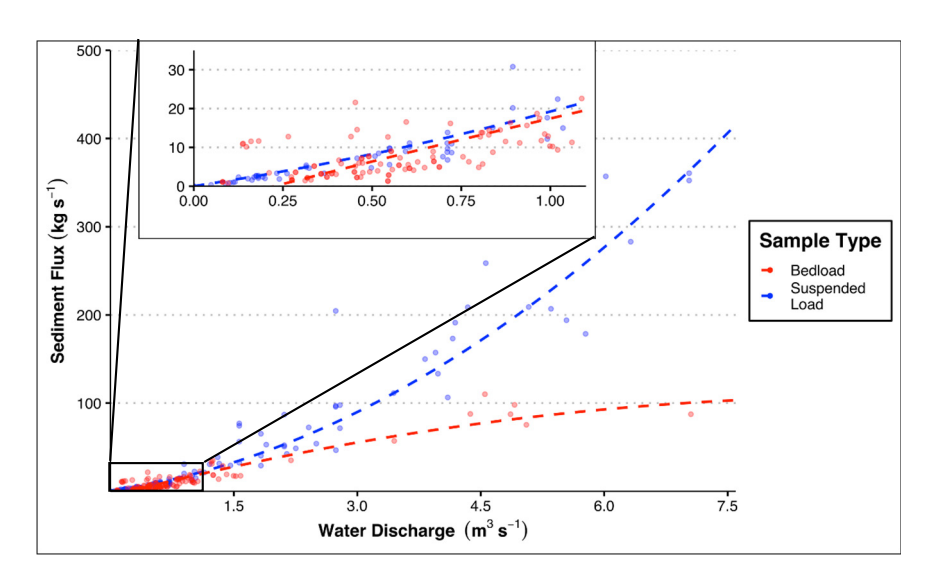


Fig. 10. Sediment flux measured at the Pinos monitoring station. At small discharges, the bedload load/suspended load ratio is near unity, decreasing as water discharge increases.

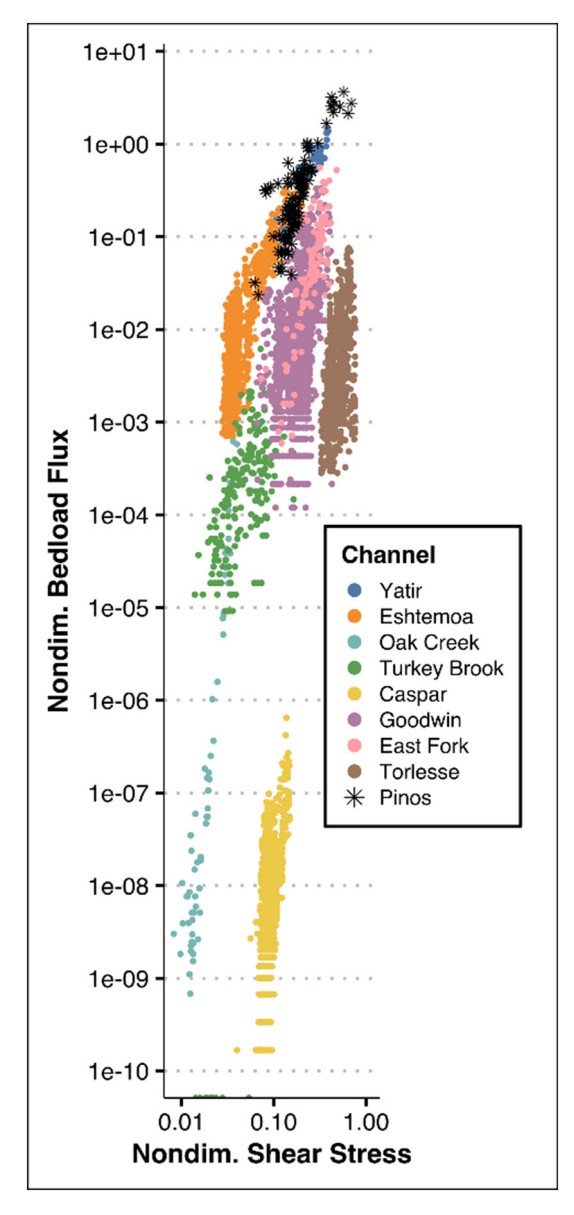


Fig. 12. Variation of nondimensional bedload flux with nondimensional shear stress for nine different rivers. Arroyo de lost Pinos samples (this study) are starred black.

suggesting that they transport bedload much more efficiently than their perennial counterparts. This topic has been explored in previous studies of ephemeral channels (e.g., Reid et al., 1995; Powell et al., 2001) and their conclusions agree with the observations made for the Pinos. The lack of an armor layer in the main channel and the transport-limited nature of the climatic setting allows the Arroyo de los Pinos to efficiently transport bedload.

Initially, we hypothesized that bedload transport in the Pinos is higher relative to other ephemeral channels because of the high sand content of the channel bed. The nondimensional bedload flux in the Pinos is indeed higher than values from the Eshtemoa, but similar rates were reported for the Nahal Yatir, a channel with a similar D_{50} (Fig. 13). They seem to be slightly more efficient at transporting bedload than the Eshtemoa, which has a larger surface D_{50} . However, these differences are smaller than we had expected, given the uniquely high sand content of the Pinos. Climatic differences produced much larger differences in bedload flux.

5. Conclusions

The Arroyo de los Pinos is a sand-rich, unarmored gravel-bed ephemeral tributary to the Rio Grande. A sediment monitoring station was constructed to quantify flow and sediment dynamics for these regimes. These first nine flow events contribute vital information on grain size, initiation of transport, and transport processes. Fundamentally, the Pinos monitoring station strives to inform regional sediment delivery to the Rio Grande, the local perennial trunk river. The majority of sediment that enters the Rio Grande is delivered by ephemeral channels such as the Pinos. Further understanding of sediment transport processes will aid regional decision makers that manage sediment within the Rio Grande. Sediment flux, especially bedload flux, is high even in very shallow flow events. The ratio between bedload and suspended load discharge reveal a dynamic system, where sand sized particles (which make up about 1/3 of bed material) are transported along the channel bed at low discharges and progressively move into suspension as water discharge increases. Data from the Pinos fills an apparent gap of high-quality gravel bed river sediment transport data. Because the channel is sand-rich, initiation of bedload transport is easier and higher rates of transport are more common. These channels produce a geomorphically significant amount of sediment despite their size and infrequency of flows. When flow events do occur, the Pinos produces some of the highest instantaneous nondimensional bedload flux yet measured in ephemeral systems.

Table 2Summary of published continuous bedload flux data.

Channel	Climate & dominant vegetation	Surface D ₅₀ (mm)	Subsurface D ₅₀ (mm)	Principal citation
Pinos (this study)	Semi-arid	4.9	6	-
	Desert shrub			
Eshtemoa	Semi-arid	20	19.5	Laronne et al. (1994); Cohen et al. (2010)
	Desert shrub			
Yatir	Semi-arid	6	10	Laronne et al. (1992); Reid et al. (1995)
	Desert shrub			
Oak Creek	Temperate	63	20	Milhous (1973)
	Forested			
Turkey Brook	Temperate	22	16	Reid and Frostick (1986)
	Grassland			
Goodwin Creek	Temperate	5.1	4.3	Kuhnle (1992); Kuhnle and Willis (1998)
	Forested/agricultural			
East Fork River	Temperate	1.5	_	Leopold and Emmett (1976)
	Grassland/forested			
Torlesse	Temperate	15	-	Hayward (1980)
	Grassland/forested			
Caspar Creek	Temperate	17	-	Richardson et al. (2020)
	Forested			

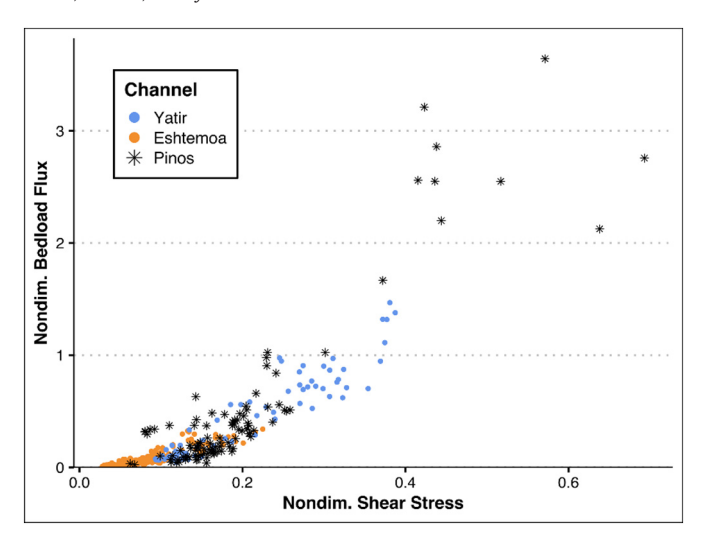


Fig. 13. The variation of bedload flux with shear stress in nondimensional space for the three ephemeral channels analyzed in this study. Bedload flux is generally higher in the Pinos and Yatir for a given shear stress.

6. Data accessibility

Data related to the Arroyo de los Pinos project are publicly available on the U.S. Reclamation Information Sharing Environment (RISE): https://data.usbr.gov/ The RISE environment provides an interactive platform for accessing data collected during Reclamation-sponsored projects. Pinos data can be accessed by searching "Arroyo de los Pinos".

Declaration of competing interest

The authors declare that they have no known competing financial interests or personal relationships that could have appeared to influence the work reported in this paper.

Acknowledgements

Multiple funding sources provided support for this research. The U.S. Bureau of Reclamation S&T program (project 9781: "Ephemeral tributary sediment transport measurement") and Albuquerque Area Office provided principal funding for construction and initial student stipends while the U.S. Army Corps of Engineers and the National Science Foundation provide current student funding. Student research grants for supplies and undergraduate research opportunities were graciously provided by the New Mexico Water Resources Research Institute and the New Mexico Geological Society.

We thank the two anonymous reviewers. Their comments greatly improved the manuscript. Special thanks to the U.S. Bureau of Reclamation and the U.S. Geologic Survey Albuquerque offices for their expertise in construction and always helpful staff. The local landowner, Mr. Bill Holmes, has always been gracious with his time and helped many of us new to the perils of flash flooding in New Mexican deserts. We thank Yaniv Munwes of Yamma Hydrometric Solutions for his considerable help in designing the equipment setup. Most importantly, thanks to the Pinos research group students: Madeline Richards, Sharllyn Pimentel, Jared Ciarico, Kelsey Romero, and Sandy Glasglo, who are always ready for long days and nights in our favorite place in the desert.

Appendix A. Supplementary data

Supplementary data to this article can be found online at https://doi.org/10.1016/j.geomorph.2021.107682.

References

Achite, M., Ouillon, S., 2007. Suspended sediment transport in a semiarid watershed, Wadi Abd, Algeria (1973–1995). J. Hydrol. 343 (3–4), 187–202. https://doi.org/10.1016/j.jhydrol.2007.06.026.

Adams, D.K., Comrie, A.C., 1997. The North American Monsoon. Bull. Am. Meteorol. Soc. 78 (10), 2197–2213. https://doi.org/10.1175/1520-0477(1997)078<2197: TNAM>2.0.CO:2.

Alexandrov, Y., Laronne, J.B., Reid, I., 2003. Suspended sediment concentration and its variation with water discharge in a dryland ephemeral channel, northern Negev. Israel. Journal of Arid Environments 53 (1), 73–84.

Alexandrov, Y., Cohen, H., Laronne, J.B., Reid, I., 2009. Total water-borne material losses from a semi-arid drainage basin: a 15-year study of the dynamics of suspended, dissolved and bed loads. Water Resour. Res. 45, W08408.

Anthony, D.J., Harvey, M.D., Laronne, J.B., Mosley, M.P., 2001. In: Anthony, D.J., Harvey, M. D., Laronne, J.B., Mosley, M.P. (Eds.), Applying Geomorphology to Environmental Management. Water Resources Publications.

Belachsen, I., Marra, F., Peleg, N., Morin, E., 2017. Convective rainfall in a dry climate: Relations with synoptic systems and flash-flood generation in the Dead Sea region. Hydrol. Earth Syst. Sci. 21 (10), 5165–5180. https://doi.org/10.3929/ETHZ-B-000199084

Bergman, N., Laronne, J.B., Reid, I., 2007. Benefits of design modifications to the Birkbeck bedload sampler illustrated by flash-floods in an ephemeral gravel-bed channel. Earth Surf. Process. Landf. 32 (2), 317–328. https://doi.org/10.1002/esp.1453.

Billi, P., 2011. Flash flood sediment transport in a steep sand-bed ephemeral stream. International Journal of Sediment Research 26 (2), 193–209. https://doi.org/10.1016/S1001-6279(11)60086-3.

Biron, P.M., Robson, C., Lapointe, M.F., Gaskin, S.J., 2004. Comparing different methods of bed shear stress estimates in simple and complex flow fields. Earth Surf. Process. Landf. 29 (11), 1403–1415. https://doi.org/10.1002/esp.1111.

Blott, S.J., Pye, K., 2001. GRADISTAT: a grain size distribution and statistics package for the analysis of unconsolidated sediments. Earth Surf. Process. Landf. 26 (11), 1237–1248. https://doi.org/10.1002/esp.261.

Buffington, J.M., Montgomery, D.R., 1997. A systematic analysis of eight decades of incipient motion studies, with special reference to gravel-bedded rivers. Water Resour. Res. 33 (8), 1993–2029. https://doi.org/10.1029/96WR03190.

Bunte, K., Abt, S.R., Asce, F., Potyondy, J.P., Ryan, S.E., 2004. Measurement of coarse gravel and cobble transport using portable bedload traps. J. Hydraul. Eng. 130 (9), 879–893. https://doi.org/10.1061/ASCE0733-94292004130:9879.

Bunte, K., Swingle, K.W., Abt, S.R., 2007. Guidelines for using bedload traps in coarse-bedded mountain streams: construction, installation, operation, and sample processing. Fort Collins, CO. https://doi.org/10.2737/RMRS-GTR-191.

Cather, S. M., & Colpitts, R. M. (2005). Geologic Map of the Loma de las Cañas Quadrangle, Socorro County, New Mexico. Socorro, New Mexico, New Mexico Bureau of Geology and Mineral Resources Open-File Digital Geologic map OF-GM 110.

Cohen, H., Laronne, J.B., 2005. High rates of sediment transport by flashfloods in the Southern Judean Desert, Israel. Hydrol. Process. 19 (8), 1687–1702.

Cohen, H., Laronne, J.B., Reid, I., 2010. Simplicity and complexity of bed load response during flash floods in a gravel bed ephemeral river: a 10 year field study. Water Resour. Res. 46 (11).

Davies-Colley, R.J., Smith, D.G., 2001. Turbidity, suspended sediment, and water clarity: a review. J. Am. Water Resour. Assoc. 37 (5), 1085–1101. https://doi.org/10.1111/i1752-1688.2001.th03624.x

De Girolamo, A.M., Pappagallo, G., Lo Porto, A., 2015. Temporal variability of suspended sediment transport and rating curves in a Mediterranean river basin: the Celone (SE Italy). Catena 128, 135–143. https://doi.org/10.1016/j.catena.2014.09.020.

Edwards, T. K., & Douglas, G. G. (1999). Field Methods for Measurement of Fluvial Sediment. Reston, VA.

Einstein, H. A. (1950). The Bed-Load Function for Sediment Transportation in Open Channel Flows, Washington, DC.

Frostick, L. E., Reid, I., & Layman, J. T. (1983). Changing size distribution of suspended sediment in arid-zone flash floods. In J. D. Collinson & J. Lewin (Eds.), Modern and Ancient Fluvial Systems (1st ed., pp. 97–106). Oxford, UK: Blackwell Publishing Ltd. doi:https://doi.org/10.1002/9781444303773.ch7.

Gomez, B., Church, M., 1989. An assessment of bed load sediment transport formulae for gravel bed rivers. Water Resour. Res. 25 (6), 1161–1186.

Groten, J.T., Johnson, G.D., 2018. Comparability of river suspended-sediment sampling and laboratory analysis methods. Scientific Investigations Report. https://doi.org/ 10.3133/sir20185023.

Habersack, H., Nachtnebel, H., Laronne, J.B., 1998. The hydraulic efficiency of a slot sampler: Flow velocity measurements in the Drau River, Austria. Gravel-Bed Rivers in the Environment, pp. 749–754.

Halfi, E., Deshpande, V., Johnson, J. P. L., Katoshevski, D., Reid, I., Storz-Peretz, Y., & Laronne, J. B. (2018). Characterization of bedload discharge in bores and very unsteady flows in an ephemeral channel. E3S Web of Conferences, 40, 02036. doi: https://doi.org/10.1051/e3sconf/20184002036.

Halfi, E., Paz, D., Stark, K., Yogev, U., Reid, I., Dorman, M., Laronne, J.B., 2020. Novel mass-aggregation-based calibration of an acoustic method of monitoring bedload flux by infrequent desert flash floods. Earth Surface Processes and Landforms https://doi.org/10.1002/esp.4988.

Hassan, M. A. (1993). Bed material and bedload movement in two ephemeral streams. In Alluvial Sedimentation (1st ed., pp. 37–49). Oxford, UK: Blackwell Publishing Ltd. doi: https://doi.org/10.1002/9781444303995.ch4.

Hassan, M.A., Schick, A.P., Shaw, P.A., 1999. The transport of gravel in an ephemeral sandbed river. Earth Surf. Process. Landf. 24 (7), 623–640. https://doi.org/10.1002/(SICI)1096-9837(199907)24:7<623::AID-ESP978>3.0.CO;2-2.

- Hayward, J. A. (1980). Hydrology and stream sediments in a mountain catchment (1st ed., Vol. Tussock Grasslands & Mountain Lands Institute, Lincoln College.
- Helley, E. J., & Smith, W. (1971). Development and calibration of a pressure-difference bedload sampler. USGS Open-File Report. doi:https://doi.org/10.3133/OFR73108.
- Kellerhals, R., Bray, D.I., 1971. Sampling procedures for coarse fluvial sediments. J. Hydraul. Div. 97 (8), 1165–1180.
- Kuhnle, R.A., 1992. Bed load transport during rising and falling stages on two small streams. Earth Surf. Process. Landf. 17 (2), 191–197. https://doi.org/10.1002/ esp.3290170206.
- Kuhnle, R.A., Willis, J.C., 1998. Statistics of sediment transport in Goodwin Creek. J. Hydraul. Eng. 124 (11), 1109–1114. https://doi.org/10.1061/(ASCE)0733-9429 (1998)124:11(1109.
- Laronne, J.B., Reid, I., 1993. Very high rates of bedload sediment transport by ephemeral desert rivers. Nature 366 (6451), 148–150. https://doi.org/10.1038/366148a0.
- Laronne, J.B., Shlomi, Y., 2007. Depositional character and preservation potential of coarse-grained sediments deposited by flood events in hyper-arid braided channels in the Rift Valley, Arava, Israel. Sediment. Geol. 195 (1–2), 21–37. https://doi.org/ 10.1016/j.sedgeo.2006.07.008.
- Laronne, J.B., Wilhelm, R., 2001. Shifting stage-volume curves: predicting event sedimentation rate based on reservoir stratigraphy. Applying Geomorphology to Environmental Management. Water Resources Publ, pp. 33–54.
- Laronne, J.B., Reid, I., Yitshak, Y., Frostick, L.E., 1992. Recording bedload discharge in a semiarid channel, Nahal Yatir, Israel. Erosion and Sediment Transport Monitoring Programmes in River Basins 210, 79–96.
- Laronne, J.B., Reid, I., Yitshak, Y., Frostick, L.E., 1994. The non-layering of gravel streambeds under ephemeral flood regimes. J. Hydrol. 159 (1–4), 353–363. https://doi.org/10.1016/0022-1694(94)90266-6.
- Laronne, J.B., Alexandrov, Y., Bergman, N., Cohen, H., Garcia, C., Habersack, H., Reid, I., 2003. The continuous monitoring of bedload flux in various fluvial environments. Erosion and Sediment Transport Measurement in Rivers: Technological and Methodological Advances. vol. 283. International Association of Hydrologic Sciences, pp. 134–145.
- Lekach, J., Schick, A.P., 1982. Suspended sediment in desert floods in small catchments. Isr. I. Earth Sci. 31 (2), 144–156.
- Leopold, L.B., Emmett, W.W., 1976. Bedload measurements, East Fork River, Wyoming. Proc. Natl. Acad. Sci. 73 (4), 1000–1004.
- Leopold, L. B., Emmett, W. W., & Myrick, R. M. (1966). Channel and Hillslope Processes in a Semiarid Area, New Mexico. Professional Paper 352-G. Washington, D.C. doi:https:// doi.org/10.3133/PP352G.
- Liébault, F., Jantzi, H., Klotz, S., Laronne, J.B., Recking, A., 2016. Bedload monitoring under conditions of ultra-high suspended sediment concentrations. J. Hydrol. 540, 947–958. https://doi.org/10.1016/j.jhydrol.2016.07.014.
- Lucía, A., Laronne, J. B., & Martín-Duque, J. F. (2011). Geodynamic processes on sandy slope gullies in central Spain field observations, methods and measurements in a singular system. Geodin. Acta, 24(2), 61–79. doi:https://doi.org/10.3166/ga.24.61-79.
- Lucía, A., Recking, A., Martín-Duque, J.F., Storz-Peretz, Y., Laronne, J.B., 2013. Continuous monitoring of bedload discharge in a small, steep sandy channel. J. Hydrol. 497, 37–50. https://doi.org/10.1016/j.jhydrol.2013.05.034.
- Malmon, D. V., Reneau, S. L., & Dunne, T. (2004). Sediment sorting and transport by flash floods. Journal of Geophysical Research: Earth Surface, 109(F2), n/a-n/a. doi:https://doi.org/10.1029/2003jf000067.
- Marra, F., Morin, E., 2018. Autocorrelation structure of convective rainfall in semiarid-arid climate derived from high-resolution X-Band radar estimates. Atmos. Res. 200, 126–138. https://doi.org/10.1016/j.atmosres.2017.09.020.
- Martín-Vide, J.P., Niñerola, D., Bateman, A., Navarro, A., Velasco, E., 1999. Runoff and sediment transport in a torrential ephemeral stream of the Mediterranean coast. J. Hydrol. 225 (3–4), 118–129. https://doi.org/10.1016/S0022-1694(99)00134-1.
- Mathys, N., Brochot, S., Meunier, M., Richard, D., 2003. Erosion quantification in the small marly experimental catchments of Draix (Alpes de Haute Provence, France). Calibration of the ETC rainfall-runoff-erosion model. Catena 50 (2–4), 527–548. https://doi. org/10.1016/S0341-8162(02)00122-4.
- Meirovich, L., Laronne, J.B., Reid, I., 1998. The variation of water-surface slope and its significance for bedload transport during floods in gravel-bed streams. J. Hydraul. Res. 36 (2), 147–157. https://doi.org/10.1080/00221689809498630.
- Milhous, R.T., 1973. Sediment transport in a gravel-bottomed stream. Unpublished PhD Dissertation. Oregon State University.
- Miwa, H., Parker, G., 2017. Effects of sand content on initial gravel motion in gravel-bed rivers. Earth Surf. Process. Landf. 42 (9), 1355–1364.
- Morin, E., Yakir, H., 2014. Hydrological impact and potential flooding of convective rain cells in a semi-arid environment. Hydrol. Sci. J. 59 (7), 1353–1362. https://doi.org/ 10.1080/02626667.2013.841315.
- Mrokowska, M.M., Rowiński, P.M., 2019. Impact of unsteady flow events on bedload transport: a review of laboratory experiments. Water 11 (5), 907. https://doi.org/10.3390/w11050907.
- Nearing, M.A., Nichols, M.H., Stone, J.J., Renard, K.G., Simanton, J.R., 2007. Sediment yields from unit-source semiarid watersheds at Walnut Gulch. Water Resour. Res. 43 (6). https://doi.org/10.1029/2006WR005692.

- Nichols, M.H., 2004. A radio frequency identification system for monitoring coarse sediment particle displacement. Appl. Eng. Agric. 20 (6), 783–787. https://doi.org/10.13031/2013.17727.
- Nichols, M.H., Stone, J.J., Nearing, M.A., 2008. Sediment database, Walnut Gulch Experimental Watershed, Arizona, United States. Walnut Gulch Experimental Watershed Water Resour. Res 44. 5–6. https://doi.org/10.1029/2006WR005682.
- Nordin, C. F. (1963). A preliminary study of sediment transport parameters, Rio Puerco near Bernardo, New Mexico. USGS Professional Paper 462. doi:https://doi.org/ 10.3133/PP462C.
- Parker, G. (1978). Self-formed straight rivers with equilibrium banks and mobile bed. Part 2. The gravel river. Journal of Fluid Mechanics, 89(1), 127–146. doi:https://doi.org/ 10.1017/S0022112078002505
- Poreh, M., Sagiv, A., Seginer, I., 1970. Sediment sampling efficiency of slots. J. Hydraul. Div. 96 (10), 2065–2078.
- Powell, D.M., Reid, I., Laronne, J.B., Frostick, L., 1996. Bed load as a component of sediment yield from a semiarid watershed of the northern Negev. Int'l Assoc. Hydrological Sciences 236, 389–398.
- Powell, D.M., Reid, I., Laronne, J.B., 2001. Evolution of bed load grain size distribution with increasing flow strength and the effect of flow duration on the caliber of bed load sediment yield in ephemeral gravel bed rivers. Water Resour. Res. 37 (5), 1463–1474. https://doi.org/10.1029/2000WR900342.
- Powell, D.M., Brazier, R., Wainwright, J., Parsons, A., Kaduk, J., 2005. Streambed scour and fill in low-order dryland channels. Water Resour. Res. 41 (5), 1–13. https://doi.org/10.1029/2004WR003662.
- Powell, D.M., Laronne, J.B., Reid, I., Barzilai, R., 2012. The bed morphology of upland single-thread channels in semi-arid environments: evidence of repeating bedforms and their wider implications for gravel-bed rivers. Earth Surf. Process. Landf. 37 (7), 741–753. https://doi.org/10.1002/esp.3199.
- Rai, A.K., Kumar, A., 2015. Continuous measurement of suspended sediment concentration: Technological advancement and future outlook. Measurement: Journal of the International Measurement Confederation 76, 209–227. https://doi.org/10.1016/j. measurement.2015.08.013.
- Recking, A., 2009. Theoretical development on the effects of changing flow hydraulics on incipient bed load motion. Water Resour. Res. 45 (4). https://doi.org/10.1029/ 2008WR006826.
- Reid, I., Frostick, L.E., 1986. Dynamics of bedload transport in Turkey brook, a coarse-grained alluvial channel. Earth Surf. Process. Landf. 11 (2), 143–155. https://doi.org/10.1002/esp.3290110205.
- Reid, I., Layman, J.T., Frostick, L.E., 1980. The continuous measurement of bedload discharge. J. Hydraul. Res. 18 (3), 243–249.
- Reid, Laronne, J.B., Powell, D.M., 1995. Bed load sediment transport in an ephemeral stream and a comparison with seasonal and perennial counterparts. Water Resour. Res. 31 (3), 773–781.
- Richardson, P.W., Seehafer, J.E., Keppeler, E.T., Sutherland, D.G., Wagenbrenner, J.W., 2020. Caspar Creek Experimental Watersheds Phase 2. https://doi.org/10.2737/RDS-2020-0018 (1985-2017).:
- Saco, P.M., Willgoose, G.R., Hancock, G.R., 2007. Eco-geomorphology of banded vegetation patterns in arid and semi-arid regions. Hydrol. Earth Syst. Sci. 11 (6), 1717–1730. https://doi.org/10.5194/hess-11-1717-2007.
- Sadeghi, S.H., Kheirfam, H., 2015. Temporal variation of bed load to suspended load ratio in Kojour River, Iran. CLEAN - Soil, Air, Water 43 (10), 1366–1374. https://doi.org/ 10.1002/clen.201400490.
- Sharma, K.D., 1996. Soil erosion and sediment yield in the Indian arid zone. International Association of Hydrologic Sciences (236), 1–8.
- Shields, A., 1936. Application of similarity principles and turbulence research to bed-load movement. Soil Conservation Service (originally in German). 26, 26.
- Tacconi, P., Billi, P., 1987. Bed load transport measurements by the vortex-tube trap on Virginio Creek, Italy. In: Thorne, C.R., Bathurst, J.C., Hey, R.D. (Eds.), Sediment Transfer in Gravel-Bed Rivers. vol. 1. Wiley, pp. 583–606.
- Teledyne, I. (2019). 3700 Portable Sampler Operation Guide. Lincoln.
- Tongway, D.J., Valentin, C., Seghieri, J., 2001. Banded Vegetation Patterning in Arid and Semiarid Environments: Ecological Processes and Consequences for Management. Springer New York.
- Wilcock, P.R., Crowe, J.C., 2003. Surface-based transport model for mixed-size sediment. J. Hydraul. Eng. 129 (2), 120–128.
- Wilcock, P.R., McArdell, B.W., 1993. Surface-based fractional transport rates: mobilization thresholds and partial transport of a sand-gravel sediment. Water Resour. Res. 29 (4), 1297–1312. https://doi.org/10.1029/92WR02748.
- Wilcock, P., Pitlick, J., & Cui, Y. (2009). Sediment transport primer: estimating bed-material transport in gravel-bed rivers. Retrieved from http://www.stream.fs.fed.us/publications/software.html.
- Wolman, M.G., Miller, J.P., 1960. Magnitude and frequency of forces in geomorphic processes. The Journal of Geology. https://doi.org/10.2307/30058255.
- WRCC. (2013). Socorro monthly climate summary. Retrieved from https://wrcc.dri.edu/cgi-bin/cliMAIN.pl?nmsoco
- Yager, E.M., Venditti, J.G., Smith, H.J., Schmeeckle, M.W., 2018. The trouble with shear stress. Geomorphology 323, 41–50. https://doi.org/10.1016/j.geomorph.2018.09.008.
- Zapico, I., Laronne, J.B., Lucía, A., Martín-Duque, J.F., 2018. Morpho-textural implications to bedload flux and texture in the sand-gravel ephemeral Poveda Gully. Geomorphology 322, 53–65. https://doi.org/10.1016/j.geomorph.2018.08.026.